

Received January 4, 2019, accepted January 15, 2019, date of publication January 25, 2019, date of current version February 22, 2019.

Digital Object Identifier 10.1109/ACCESS.2019.2895129

# PRDL: Relative Localization Method of RFID Tags via Phase and RSSI Based on Deep Learning

LEIXIAN SHEN<sup>1</sup>, QINGYUN ZHANG<sup>1</sup>, JIAYI PANG<sup>1</sup>, HE XU<sup>1,2</sup>, AND PENG LI<sup>1,2</sup>

<sup>1</sup>School of Computer Science, Nanjing University of Posts and Telecommunications, Nanjing 210023, China

<sup>2</sup>Jiangsu High Technology Research Key Laboratory for Wireless Sensor Networks, Nanjing 210003, China

Corresponding author: He Xu (xuhe@njupt.edu.cn)

This work was supported in part by the National Key R&D Program of China under Grant 2018YFB1003201, in part by the CERNET Innovation Project under Grant NGII20180605, in part by the National Natural Science Foundation of China under Grant 61572260, Grant 61672296, Grant 61602261, and Grant 61872196, in part by the Jiangsu Natural Science Foundation for Excellent Young Scholars under Grant BK20160089, in part by the Scientific and Technological Support Project of Jiangsu Province under Grant BE2016185, Grant BE2016777, and Grant BE2017166, in part by the STITP of the Nanjing University of Posts and Telecommunications (NUPT) under Grant SZDG2018014, and in part by the 1311 Talent Plan of the Nanjing University of Posts and Telecommunications (NUPT).

**ABSTRACT** Ultra-high frequency radio frequency identification (UHF RFID) technology has been widely used in many areas, and RFID localization becomes a research hotspot. There are many kinds of research on absolute localization; however, due to some disadvantages of absolute localization, relative localization is more effective in some situations. At present, there are some problems with relative localization: existing methods have low localization accuracy, and it is difficult for them to deal with high-density tags. Aiming at these problems, this paper proposes PRDL: relative localization method of RFID tags via phase and RSSI based on deep learning. By using deep learning, the variation characteristics of RFID phase and RSSI are extracted with limited data accuracy conditions. On this basis, we can infer the relative positional relationship of RFID tags with high accuracy, and design the corresponding sorting algorithm to obtain the sequence arrangement. PRDL has experimented with bare tags and actual books, and the experimental results show that PRDL can achieve better results than the traditional relative localization methods. A series of tests also showed that PRDL has good robustness and generalization ability.

**INDEX TERMS** Relative localization, RFID, deep learning, RSSI, phase.

## I. INTRODUCTION

Ultra-high frequency Radio Frequency Identification (UHF RFID) technology has been widely used in many areas, such as logistics, clothing industry, library management, warehouse management and so on, and object localization has always been a hot topic in RFID research. Localization can be divided into absolute localization and relative localization. The absolute position of an object refers to its coordinate value in a coordinate system and the relative position of an object refers to its order with respect to other objects.

Most of previous research is aimed at absolute localization, but in many situations, the relative position of an object is more important than its absolute position. For example, in the library, when librarians are looking for misplaced books, they need to know the current order of books rather than their coordinates; In a conveyor system, the order of the objects

provides enough information, and absolute position is not important.

There are three main reasons why absolute localization is not suitable for these scenes. First, the error of absolute localization is relatively large, and it is difficult to complete the localization of objects with small spacing. For instance, the RFID indoor absolute localization scheme proposed by Wang *et al.*, achieves the accuracy of 11 cm in the library [11], a relatively good outcome, but the distance between books is much smaller than 11 cm, so some absolute localization schemes can hardly determine the sequence of books because of their inadequate accuracy. Second, although absolute localization method [1] can reach millimeter level, but it uses four reader antennas, which is not only hardware costly, but also inconvenient to use. Third, absolute localization usually requires multiple reader antennas to be placed at fixed locations, and if someone passes or interferes with the running localization system, the localization results will be hugely influenced.

The associate editor coordinating the review of this manuscript and approving it for publication was Prakasam Periasamy.

To some extent, relative localization is easier than the absolute localization because it is committed to find out the relative position between objects rather than the coordinates. However, there are still many research difficulties in relative localization. First, for practical use, the accuracy of localization must be guaranteed. Absolute localization methods position objects respectively, different with relative localization. In relative localization, the positioning deviation of one object will affect the positioning result of other objects, which means high accuracy of relative localization is hard to achieve. Second, localization methods should have high fault tolerance (robustness). When moving the reader antenna to collect data, it is difficult to control parameters such as the moving speed, the distance between antenna and tags, etc., so the robustness is a very important indicator of the localization method.

In recent years, deep learning, an algorithm that attempts to abstract data with multiple processing layers consisting of complex structures or multiple nonlinear transforms, is continuously combined with practical applications to further improve the accuracy and efficiency of applications [14]–[16]. Nevertheless, there are very little applications combined deep learning with RFID localization, let alone relative localization. In view of the above situation, this paper puts forward PRDL: Relative Localization Method of RFID Tags via Phase and RSSI based on Deep Learning. Using commercial off-the-shelf (COTS) RFID readers and passive tags, PRDL employs deep learning to extract information from the variation of RFID phase and RSSI, and determines the location and the order of RFID tags with high accuracy. Holding the antenna in hand or clamping them by instrument, we scanned the aligned RFID tags evenly along a dimension in one direction and collected relevant data. Small spacing between tags (only 1–3 cm), measurement errors, etc. make collected data entangled. But these data show obvious change characteristics, indicating location information. According to the Otrack phenomenon and our observations, when we move the antenna along a dimension in one direction, as the distance between the antenna and the tag decreases first and then increases, the RSSI of the tag decreases first and then increases in proportion to the distance, and becomes the minimum when the reader is perpendicular above the tag along that dimension, and the phase also changes significantly with the movement of the antenna [9]. We trained the machine to analysis the dynamic data and find the current order of tags. To know the order of the tag sequence, we just need to know the left-right relationship between any two tags. We collected a large amount of training data, labeled every two tags with their correct left-right relationship. Then the training data was input into the deep neural network which is constructed in this paper, and the model output by deep neural network is used to obtain the left-right relationship between any two tags of an unknown tag sequence. After that, the order of the sequence was derived from left-right relationships by using a sort algorithm and was visualized. After studying the bare tag sequence, we applied PRDL to the

book arrangement. The experimental result shows that PRDL can achieve high accuracy and good robustness.

The main contribution of this paper is to apply deep learning technology to the relative localization of RFID tags, breaking through the problem of relative localization under the condition of high-density RFID tags. Even if the tags are densely arranged, for example when the distance between tags is 1 cm, PRDL can still achieve good results, thereby increasing the relative localization accuracy to a new level. In addition, PRDL better handles the robustness of relative localization and solves the problem that the existing technology has a severe fluctuation in accuracy as the spacing between tags decreases.

This paper not only provides a new method for relative localization, but also combines deep learning technology and the Internet of Things to provide a new idea for the solution of related IoT problems, and enriches the application of deep learning technology.

The rest of paper is organized as follows. In Section II, a review of related research about RFID location is provided. In Section III, we discussed some preparations and attempts before the experiment. In Section IV, we introduce the design details of our PRDL based relative localization system. The experiments and evaluation are illustrated in Section V. Finally, we conclude this paper in Section VI.

## II. RELATED RESEARCH

This section discusses the researches on absolute localization and relative localization, then analysis their existing drawbacks.

**Absolute localization:** In recent years, the localization technology of RFID has been continuously improved, and the positioning accuracy is constantly increasing. Landmarc was the first mature RFID localization system based on Received Signal Strength Indication (RSSI) [2], later many researchers ameliorated it. Zhang *et al.* [3] introduced quantum particle swarm optimization cubature Kalman filter which makes the average localization accuracy approximately 17.5 cm; Xu *et al.* [4] improved the Landmarc with SVM and the localization accuracy is about 19 cm. Meanwhile, localization methods and algorithms based on Time of Arrival (TOA), Time Different of Arrival (TDOA), Angle of Arrival (AOA), and Phase come out. Fu *et al.* [5] proposed a method for the localization of moving object based on UHF RFID Phase and Laser Clustering and it achieves approximately 25 cm localization accuracy; Ma *et al.*'s [6] localization algorithm based on AOA and PDOA can achieve decimeter accuracy. In addition, Zhang *et al.* [7] presented the Bayesian filter of variable RF transmission power (BFVP), and its localization accuracy is less than 0.5 m in the actual retail environment; Wang *et al.* [11] introduced the first fine-grained RFID positioning System that is robust to multipath and non-line-of-sight scenarios, and the test accuracy in the library is about 11 cm; Duan *et al.* [8] put forward a fast and easy method called Tagspin to accurately locate the reading using COTS tags, and the average accuracy in three-dimensional space

is getting to 7.3 cm; “Differential Augmented Hologram” was proposed by Yang *et al.* [1], which even improves the positioning accuracy to the millimeter level.

Relative localization: At present, the research results of localization based on phase are not fruitful enough, where existing many breakthroughs. Shangguan *et al.* [9] first discovered the Otrack phenomenon, a critical region of reading rate when a tag gets close enough to a reader. After an in-depth study, they presented the first study of relative object localization ‘Spatial-Temporal Phase Profiling-Based Method for Relative RFID Tag Localization (STPP)’. The ordering accuracy of STPP for misplaced books is about 84% and 95% for baggage handling [10]. Wang *et al.* came up with a relative localization method based on RSSI and human motion (HMRL), which is efficient and convenient to deploy and the accuracy can reach 90%-95% [12]. In addition, Nick T *et al.* used an unscented Kalman Filter with relative position information for localization of passive UHF RFID labels [13]. STPP and HMRL focus on relative object localization in a two dimensional space by moving the antenna only once, respectively calculating the accuracy of the two dimensions on the X and Y axes. The common drawback of these methods is that the accuracy is not particularly high, and it is difficult to process high-density tags.

According to relevant research status, we proposed a relative localization method of RFID tags via phase and RSSI based on Deep Learning (PRDL) to improve the accuracy of relative localization in one dimension, equivalent to X latitude in STPP and HMRL. When the distance between objects is large, it is easy to distinguish the relative positional relationship, while when the distance is small, it is very difficult. So we focus on the relative localization of high-density tags in one dimension.

### III. EXPERIMENTAL PREPARATION

This section discusses experiment preparations, including RFID tags processing, data collecting, preliminary data analysis and the inference about the appropriate localization method. The symbols used in this paper and descriptions are shown in Table 1.

#### A. LABORATORY EQUIPMENT PREPARATION

The process of reading RFID tag is affected by many factors, including signal propagation medium, angles of the reflected signal of tags, obstacles around tags, etc. We used H47 passive tags in the initial experimental stage. After eliminating various interference factors, we found that tags were easily bent, which had a great influence on the collected data, therefore a set of acrylic board laboratory equipment was designed. As shown in Figure 1, the acrylic boards are made of plastic, and the influence of those dielectric coefficient on the RFID signal is within the controllable range. Using two acrylic plates to sandwich one RFID tag can well eliminate the influence of the tag bending on the data.

TABLE 1. Main notations.

| Symbols                            | DESCRIPTIONS   |
|------------------------------------|--|
| $d$                                | distance between transmitter and receiver  |
| $d_0$                              | reference path loss at the close distance  |
| $X_\sigma$                         | normal random variable, standard deviation is $\sigma$   |
| $\theta$                           | measured phase   |
| $\theta_T, \theta_R, \theta_{Tag}$ | phase shifts   |
| $K_e$                              | effective aperture   |
| $P_{out}$                          | output power   |
| $P_{in}$                           | input power  |
| $\lambda$                          | Wavelength   |
| $g$                                | the ratio of the amplitude of the reflected wave to the amplitude of the original electromagnetic wave |
| $\delta$                           | phase difference   |
| $L$                                | distance scanned by antenna  |
| $S$                                | distance between tags  |
| $N$                                | numbers of tags  |
| $P, P_s$                           | Phase, standardized Phase  |
| $T, T_d, T_s$                      | Timestamp value, standardized Timestamp value  |
| $C_{ij}$                           | confidence of the i-th tag is on the right side of the j-th tag  |
| $A$                                | matrix of confidence   |
| $w$                                | weight   |
| $b$                                | bias   |
| $O$                                | output value   |



FIGURE 1. Acrylic board laboratory equipment.

#### B. CHANGES IN RSSI DURING ANTENNA MOVEMENT

Received Signal Strength Indication (RSSI) is an indication of the received signal strength, an optional part of the wireless transmission layer, used to determine the quality of the link, and whether to increase the broadcast transmission strength. A RSSI value (dBm) is negative and its maximum is 0.

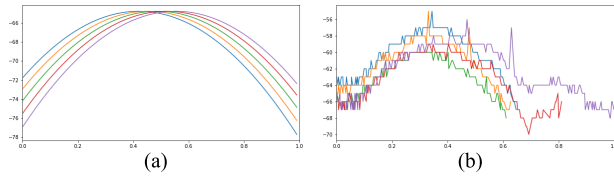


FIGURE 2. Theoretical and actual maps of RSSI changes.

Only under the ideal condition the RSSI value of a tag can be 0, meaning that the tag receives all signals from the antenna. Ideally, when the antenna scans through a sequence of tags, RSSI values of tags are periodic and hierarchical. As shown in Figure 2(a), there are five different colored lines, each representing a tag, and the left-right relationship of any two tags can be directly distinguished by the figure. In fact, RSSI is affected by distance, medium and other factors, and many studies have shown that the RSSI indoor path loss follows the log-distance path loss model [17], [18]:

$$PL(d)(dB) = PL(d_0) + 10n \lg(d/d_0) + X_\sigma, \quad X_\sigma \sim N(0, \sigma) \quad (1)$$

where  $PL(d)$  is the path loss when the distance between transmitter and receiver is  $d$ , and  $PL(d_0)$  is the reference path loss at the close distance, which is obtained by actual test.  $n$  is the path loss factor related to the surrounding environment.  $X_\sigma$  is a normal random variable with a standard deviation of  $\sigma$ . Affected by various factors, the data for each tag is interlaced, and the amount of data measured by different tags is different, even some tags have data missing, so it is difficult to directly judge two tags' left-right relationship through visualization. The actual scan result is shown in Figure 2 (b), and the data shown in the figure is part of the data collected by the antenna scanning through 20 tags in Figure 1.

### C. CHANGES IN PHASE DURING ANTENNA MOVEMENT

Phase is one of the basic properties of a signal, ranging from 0 to 360 degrees, and the phase value of the RFID signal describes the extent to which the received signal is offset from the transmitted signal. The measured phase value output by the reader is a periodic function and can be expressed as:

$$\theta = \left( 2\pi \frac{2d}{\lambda} + \theta_T + \theta_R + \theta_{Tag} \right) \bmod 2\pi \quad (2)$$

where  $d$  is the distance between the reader antenna and the tag;  $\lambda$  is the wavelength; the round-trip distance for a signal from transmitter to receiver is  $2d$ ;  $\theta_T$ ,  $\theta_R$ , and  $\theta_{Tag}$  are the phase shifts introduced respectively by the reader's transmitter circuit, the reader's receiver circuit, and the reflective characteristics of the tag [10]. Like RSSI, the actual value of the phase differs greatly from the theoretical value and the data of each tag is interlaced and even some data is missing. As shown in Figure 3, the source of the actual data is the same as the RSSI data source of part B.

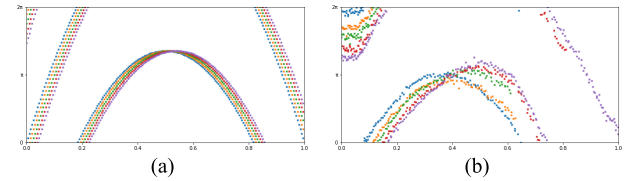


FIGURE 3. Theoretical and actual maps of phase changes.

### D. DATA FLUCTUATION

Considering the path loss of the reader energy, the simplest case is to assume that the antenna radiates energy uniformly in all directions of the space and is represented in space as a spherical body of radius  $r$ . And the energy actually received by the tag is proportional to the energy density across the tag antenna in the area. Therefore, for an antenna with an effective aperture of  $K_e$ , when a plane wave having an energy density of  $\rho$  is received, the actually received energy is  $\rho K_e$ . The energy density at the distance  $r$  is the ratio of the transmitted energy  $P_T$  to the spherical surface, so the energy  $P_R$  received at the tag is:

$$P_R = P_T \frac{K_e}{4\pi r^2}, \quad K_e = \frac{\lambda^2}{4\pi}$$

where  $\lambda$  is the wavelength of the corresponding frequency signal. The energy change in this ideal state is regular, but the transmission space environment between the reader and the tag is much more complicated in reality. The multipath effect and existence of the ionizer make actual energy changes difficult to quantify and describe. A series of issues such as attenuation, tag decoding capability and environmental impact are all related to RFID recognition performance [30]–[33]. This makes it impossible to obtain ideal RSSI and Phase data.

The interference signal formed by the signal of the reader after scattering and reflection is not a simple energy superposition at the receiving end, but an accumulation of potentials at each point. For example, the electromagnetic wave emitted by the reader is superimposed with two reflected waves, and the energy of the reflected wave is 1/10 of the original electromagnetic wave, so the superposed potential obtained is:

$$G_s \cos(\omega t) = g_o \cos(\omega t) + g_{r1} \cos(\omega t + \delta_1) + g_{r2} \cos(\omega t + \delta_2) \quad g_o = 1, g_{r1} = g_{r2} = \frac{1}{\sqrt{10}}$$

where  $g$  is the ratio of the amplitude of the reflected wave to the amplitude of the original electromagnetic wave,  $\delta$  is the phase difference between the reflected wave and the original electromagnetic wave, and the phase difference depends on the transmission distance of the electromagnetic wave. When the length is increased by 1/4 of the wavelength, the phase is changed by  $\pi/2$ , and this small change is difficult to control in reality [30]–[33]. Consider the case where the phase difference is 0 and  $\pi$ , respectively, and convert the result into a decibel value in communication engineering.

$$V_{dB} = 10 \lg \frac{P_{out}}{P_{in}}$$

where  $P_{out}$  is the output power,  $P_{in}$  is the input power. When the phase difference is 0:

$$G_s = g_o + \frac{g_o}{\sqrt{10}} + \frac{g_o}{\sqrt{10}} \approx 1.632g_o$$

$$\frac{P_{out}}{P_{in}} = \left(\frac{G_s}{g_o}\right)^2 \approx 2.7 = 4.27dB$$

The energy obtained at this time is 4.27 dB higher than the original electromagnetic wave. When the phase difference is  $\pi$ , it can be similarly calculated:

$$G_s = g_o - \frac{g_o}{\sqrt{10}} - \frac{g_o}{\sqrt{10}} \approx 0.368g_o$$

$$\frac{P_{out}}{P_{in}} = \left(\frac{G_s}{g_o}\right)^2 \approx 0.14 = -8.69dB$$

The energy obtained at this time is 8.69dB lower than the original electromagnetic wave, so that the difference can reach  $4.27+8.69 = 12.96dB$ . This energy attenuation due to position or frequency offset is very significant in RFID systems, and in relative localization, a large number of dense tags are involved. Mutual influence between the tags is very serious. We fixed the reader antenna and 20 densely packed tags, collect data statically, and take the RSSI and Phase data of a tag as shown in Figure 4. It can be seen that data collected from static tags will also fluctuates.

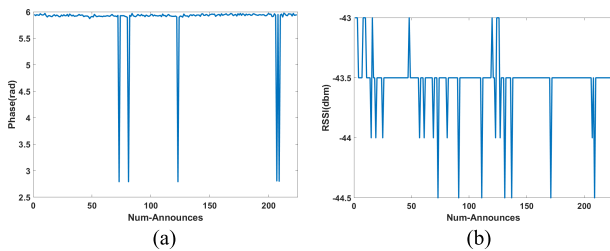


FIGURE 4. RSSI and Phase fluctuations.

**E. ANALYSIS AND CONJECTURE**

Figure 2 and Figure 3 respectively describe the theoretical and actual changes of RSSI and phase. It is possible to try to calculate the relative position directly by some algorithms, but the mismatch between the data will cause a large error. As analyzed in Part D, data is inevitably fluctuating, and it is obviously not good enough to represent a tag with a single attribute value. STPP also mentions that when the tag arrangement is too dense, every two tags will form two identical circular loops, which will generate inductive coupling effect. The tags will be shadowed by each other, resulting in low reading rate. So the serialized data is used can to compensate for the reading rate. It will not have a big impact even if there is some data fluctuations, avoiding using filtering algorithms. And there is more information for model to extract features. It can be clearly seen that the RSSI and phase of different tags have obvious variation tendency, and the overall picture is very layered, so we suspect that the characteristics of the variation can be extracted through deep learning, and the

model of the variation tendency can be trained. It can be seen from the figure that both RSSI and Phase data can reflect the characteristics of each tag when the antenna moves, so both RSSI and Phase are selected as part of the training data. We consider that the experiment on equally spaced bare tags should be carried out first. In the experiment, we use antenna scans dozens of data as training data, so that the preliminary model is outputted, then the model can be applied to the actual scene of books where each book is labeled with a passive RFID tag. Because the distance between the books is not equal, the effect of the preliminary model should be slightly worse. To solve this problem, data with different tag spacing needs to be added to the training data to increase the generalization ability of the model. After the model accuracy is stable, the speed, distance and other factors should be considered, that is, by further increasing the training data to optimize the model and enhance the robustness of the system.

**IV. SYSTEM DESIGN**

This section elaborates the implementation details of PRDL, including data acquisition and preparation, deep neural network construction, and sorting algorithm design.

**A. SYSTEM ARCHITECTURE**

Fig. 5 outlines the work flow of PRDL. When starting to collect RFID data, the user can control the reader through the database server, and the reader sends an instruction to the antenna to transmit the electromagnetic wave to the tag monitoring area. Then the user sweeps the tags evenly with the antenna. After the tags receive the electromagnetic wave, they transmit their own information (including RFID antenna Port, EPC Number, RSSI, phase, Timestamp etc.) back to the reader through the antenna to be stored in the database. After getting a large amount of dynamic data, the server reads and processes the real-time electromagnetic data from the database, inputs the training data into the deep neural network, outputs the model. Finally, the test data is read to input the model, and the result is output.

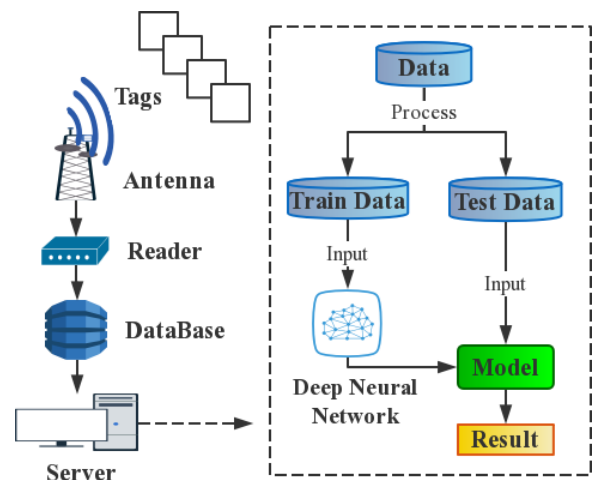
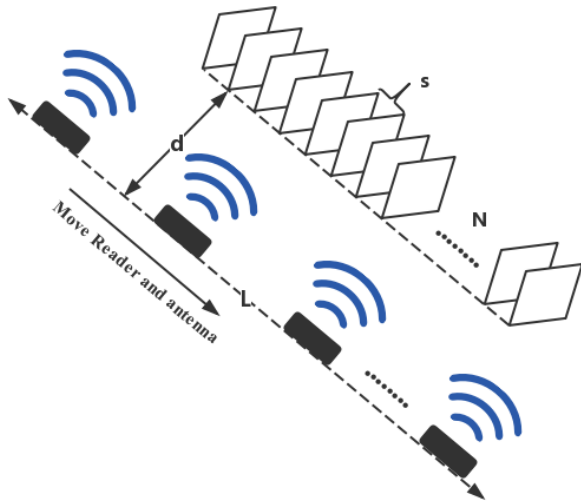


FIGURE 5. System work flow.

**B. DATA ACQUISITION AND PREPARATION**

Stably and evenly moving the antenna to scan tag sequence along a dimension in one direction, as shown in Figure 6, where  $N$  is the number of tags,  $s$  is the distance between the tags,  $d$  is the distance between the antenna and the tag, and the distance scanned by antenna is  $L$ . Define one piece of data collected from a tag as ERPT-File (EPC-RSSI-Phase-Timestamp File), ERPT-File includes EPC (Electronic Product Code), RSSI, Phase and Timestamp, and process the data as follows [19].



**FIGURE 6. Data collection.**

The data range of Phase is  $[0, 2\pi]$ , which is standardized by dividing each data  $P$  by  $2\pi$ :

$$P_s = \frac{P}{2\pi} \tag{3}$$

The Timestamp value is large, and each data  $T$  is standardized:

$$\begin{aligned} T_d &= T - \min(T) \\ T_s &= \frac{T_d}{\max(T_d)} \end{aligned} \tag{4}$$

In order to distinguish left-right relationships between the tags, in the experiment, the last digit of every EPC was set to be  $1-N$  and was called the serial number. The speed of the antenna sweeping the label is about 13-15cm/s. For example, in the early stages of the experiment, we set  $d$  to 35 cm,  $L$  was 120 cm, and the antenna scan time was about 8-9s, so that an average of 2500-3500 ERPT-Files can be collected per scan, and an average of 100-200 ERPT-Files can be collected per tag in one scan. The ERPT-File for each tag is sorted by timestamp and placed in a sequence of length 250. The portion of ERPT-File with less than 250 is padded with 0, indicating that no data is detected, thus sequence data of  $n$  tags are obtained.

Each two tag sequences can form a pair of data, and the tag with a small serial number is known to be on the left side of the tag with a large serial number, so that a training data

can be formed, and label is the left-right relationship of the two tags. Scanning  $n$  tags for  $m$  times,  $m \times C_n^2$  training data can be obtained, and the amount of data collected by us is very impressive, which ensures the data foundation of the accuracy and stability of the subsequent training model. Since the data collected by the RFID system is greatly affected by the environment, including tag placement status, computer status, laboratory environment, etc., we collect data in different time periods and reposition the experiment tags each time, thus enhancing the generalization of the model, and avoid data over-fitting.

**C. DEEP NEURAL NETWORK**

The data collected is serialized whose phase and RSSI change with time, so Long Short-term Memory (LSTM) should be a suitable network model. However, in our experiment, we found that Convolutional Neural Network (CNN) is far better than LSTM, which may be due to CNN's better extraction of features. We refer to the idea of convolutional recurrent neural network(CRNN), use CNN to extract the feature, and then pass it to LSTM [27]–[29]. However, in this case, CNN has achieved extremely high accuracy and it is difficult to compare the advantages of CRNN. For the comprehensive consideration of detection speed and equipment cost, we chose deep neural network based on CNN.

CNN is a feedforward neural network, which is widely used in the field of image recognition and has significant benefits [20]–[22]. Its weight-sharing network structure makes it more similar to biological neural networks, reducing the complexity of the network model and the number of weights, and it mainly includes convolutional layers and pooling layers. For the convolutional layer, the input data shape is  $(n, \text{channel}, A, B)$ ,  $n$  is the number of samples, and channel is the number of channels. For each channel, each filter, the convolution operation is shown in Figure 7.

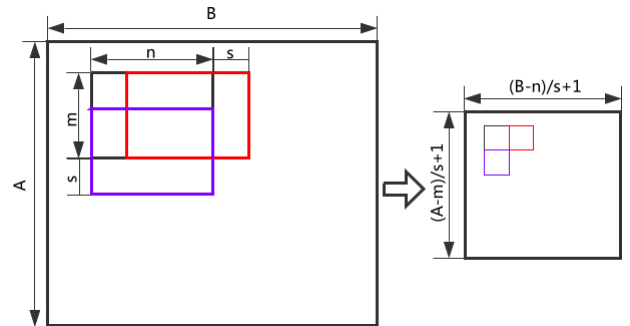


**FIGURE 7. Convolution operation.**

Filter size is  $m \times n$ , and the stride is  $s$ . For each input corresponding to the filter size, multiply each value  $x$  in the area and weight  $w$ , then plus bias  $b$ , and  $O$  is the output:

$$O_{i,j} = \sum_{p=0}^m \sum_{q=0}^n x_{is+p,js+q} w_{is+p,js+q} + b \tag{5}$$

The operation process of pooling layer is similar to the convolutional layer, except that feature map is usually non-overlapping partitioned by pooling layer, which means  $m = n = s$ . The process of pooling layer operation is shown in Figure 8.

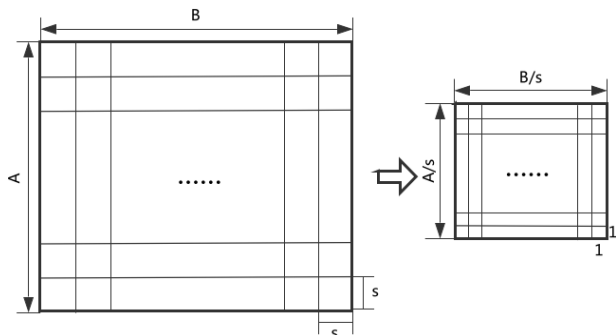


FIGURE 8. Pooling layer operation.

This paper uses max pooling, the output is the maximum value in the calculation area, and the calculation formula is:

$$O_{i,j} = \max\{x_{is+p,js+q} | p \in (0, 1, \dots, m), \quad q \in (1, 2, \dots, n)\} \quad (6)$$

In terms of activation function, the Sigmoid function is used in the last layer of the network, and the other layers use tanh.

The Softmax function compresses the vector to the range of [0, 1] proportionally and guarantees that the sum of all elements is 1. As well known that the Softmax function has a wide range of applications in classification problems. The function expression is as shown in formula 8, where K is the number of classifications. The probability P of the input sample x belonging to the jth class is shown in the following formula.

$$\tanh(x) = \frac{e^x - e^{-x}}{e^x + e^{-x}} \quad (7)$$

$$\sigma(z)_j = \frac{e^{z_j}}{\sum_{k=1}^K e^{z_k}}, \quad j = 1, \dots, K. \quad (8)$$

$$P(y = j|x) = \frac{e^{x^T w_j}}{\sum_{k=1}^K e^{x^T w_k}} \quad (9)$$

Sigmoid is a special case of Softmax at  $K = 2$ . Here we just need to distinguish the left and right relations of the two labels, so the model only needs to perform binary classification, and the last layer of the network uses the Sigmoid function.

$$Sigmoid(x) = \frac{1}{1 + e^{-x}} \quad (10)$$

In the practice of this paper, the input data is (n, 3, 2, 250), as Figure 9 shows. Each piece of data contains information of two tags a, b, and the three layers of channels are timestamp, phase, and RSSI. The maximum length of each data is 250,

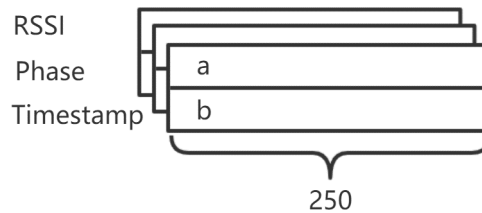


FIGURE 9. The structure of training data.

which is related to the actual data obtained under our experimental conditions and can be adjusted according to the actual situation.

Through five convolution layers, one max pooling layer, two fully connected layers and some dropout layers, final output is the label, whether a is on the left side of b. The neural network is shown in Figure 10.

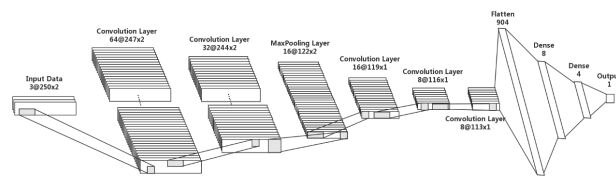


FIGURE 10. Deep neural network structure based on CNN.

D. SORTING ALGORITHM

Enter the relevant data of the two tags a, b into the model and output a number C which is between 0 and 1 to reflect the confidence that the a tag is on the left side of the b tag. It is generally believed that if  $C_{ij} < 10^{-4}$ , then the i-th tag is on the right side of the j-th tag; if  $C_{ij} > 1 - 10^{-4}$ , then the i-th tag is on the left side of the j-th tag. For instance, if you get  $C_{2,3} = 0.61$ , the model considers that the probability of 2th tag on the left side of 3th tag is 61%. And  $C_{ij} + C_{ji} = 1$  is not necessarily true, because the model cannot recognize that a-b and b-a are two arrangement of tag a and b, and it will only judge the relationship between two tags based on the input data. Then for n test tag sequences, an  $n \times n$  matrix A can be obtained, where:

$$A_{ij} = \begin{cases} 0, & i = j \\ C_{ij}, & else \end{cases} \quad (11)$$

Obviously, the error of predicting the first tag to the tenth position is much larger than the error of predicting it to the second position. Meanwhile, the smaller the difference in the serial number between the correct position and the predicted position in the sequence, the smaller the localization error. Therefore, the concept of the sorting error is defined as follow. The weight of each number in the matrix is the absolute value of the difference between its row number and column number, so in each column of the weight matrix, the weight value on the main diagonal is the lowest, and increases symmetrically to both sides. Moreover, each column of the matrix A represents the confidence of the

left-right relationships between a tag and other tags. Consequently, sorting error of each tag is the sum of product of each confidence in its column and the corresponding weight, and the algorithm for computing sorting error is shown in Algorithm 1.

---

**Algorithm 1** ComputeError(A,j)
 

---

**Initialize** Error = 0;  
**Input:** matrix A(N × N), column number j  
**Output:** Error  
**for** i = 0 to N-1 **do**  
     Error += |j-i|\*A<sub>ij</sub>;  
**end**  
**return** Error;

---

In theory, the matrix A' formed correctly by the sequence should be:

$$A' = \begin{bmatrix} 0 & 1 & \dots & 1 & 1 \\ 0 & 0 & \dots & 1 & 1 \\ \vdots & \vdots & \ddots & \vdots & \vdots \\ 0 & 0 & \dots & 0 & 1 \\ 0 & 0 & \dots & 0 & 0 \end{bmatrix}$$

Exchange the data of the p-th and q-th rows, the data of the p-th and q-th column of the actual matrix A, to exchange the positions of the p-th and q-th tag, and repeat this operation to make A approximate A'. According to the definition of the sorting error, using the idea of bubble sorting, sort the data to get the correct sequence.

Assume that the actual order of the tags is [1]–[5], the weight matrix W(N = 5) at N = 5 and the judgment matrix A (N = 5) of the model output are as follows:

$$W(N = 5) = \begin{bmatrix} 0 & 1 & 2 & 3 & 4 \\ 1 & 0 & 1 & 2 & 3 \\ 2 & 1 & 0 & 1 & 2 \\ 3 & 2 & 1 & 0 & 1 \\ 4 & 3 & 2 & 1 & 0 \end{bmatrix} A(N = 5) = \begin{bmatrix} 0 & 0.42 & 0.93 & 0.96 & 0.97 \\ 0.07 & 0 & 0.84 & 0.93 & 0.96 \\ 0.09 & 0.11 & 0 & 0.92 & 0.92 \\ 0.06 & 0.05 & 0.05 & 0 & 0.66 \\ 0.04 & 0.04 & 0.03 & 0.03 & 0 \end{bmatrix}$$

It can be seen from the matrix that the model misjudges the relationship between tag NO. 1 and tag NO. 2.  $C_{1,2} = 0.42$  indicates that the model considers that the confidence probability of tag NO. 1 on the left side of tag NO. 2 is only 42%, and other numbers in matrix A are consistent with the actual situation. The matrix is processed using the sorting algorithm (Algorithm 1 & 2) in PRDL, where ComputeError(A, 0) gets the ERROR of tag NO. 1:  $0 \times 0 + 1 \times 0.07 + 2 \times 0.09 + 3 \times 0.06 + 4 \times 0.04 = 0.59$ , ComputeError(A, 0) gets the ERROR of tag NO. 2:  $1 \times 0.42 + 0 \times 0 + 1 \times 0.11 + 2 \times 0.05 + 3 \times 0.04 = 0.75$ . According to the result of the algorithm,  $0.59 < 0.75$ , so the tag No. 1 is on the left side of the tag No. 2, so do not

---

**Algorithm 2** Sort(A)
 

---

**Input:** matrix A(N × N)  
**Output:** array Q, the order of books  
**for** i = 0 to N-2 **do**  
     **for** j = 0 to N-2-i **do**  
         **if** ComputeError(A,j) > ComputeError(A,j + 1) **then**  
             exchange column j with column j + 1 in matrix A;  
             exchange row j with row j + 1 in matrix A;  
             exchange Q[j] with Q[j + 1];  
         **end**  
     **end**  
**end**  
**return** Q;

---

interchange the positions of the two tags, and so on. Finally, the tag order Q [1]–[5] is obtained, which is consistent with the actual order.

This example shows that PRDL can basically obtain the order of tags through the judgment matrix, and can reduce the influence of misjudgment in the judgment matrix through the sorting algorithm. Mainly because when determining the position of a tag, the model outputs the relative positional relationship of each tag to other tags, so that the amount of information used for sorting is sufficient, instead of just considering the single attribute value of each tag itself as in the existing algorithm. And the sorting algorithm reasonably assigns a weight matrix to the judgment matrix.

## V. SYSTEM EVALUATION

### A. HARDWARE AND SOFTWARE

The reader used in our system is provided by Impinj, Speedway Revolution R420, including an E9208PCRN F UHF antenna and a set of H47 UHF passive tags [23]. The communication frequency between reader and tags is between 902MHz-928MHz. The reader is connected to the router through WiFi. So we can connect the computer to the reader via WiFi wirelessly, then get the data obtained by the reader directly on the computer.

We programed in python 3.6, using python packages including tensorflow-gpu 1.1.0, keras 2.1.2, numpy 1.12.1, pandas 0.23.0, matplotlib 2.2.2, etc. The program is executed on a Shinelon PC equipped with an Intel(R) Core(TM) i7-6700HQ CPU (2.60 GHz, 4 cores), a GTX1060 6G GPU and 16 GB RAM.

### B. DEPLOYMENT

We first experiment on the bare tags, get the initial model and deploy it to the actual application scenario of the book.

The experimental scene of bare tag is shown in Figure 11 (a). In order to obtain consistent data for comparison, the number of tags is set to 20, the distance between the tags is 2 cm, the reader is 35 cm away from the tag sequence, the lowest



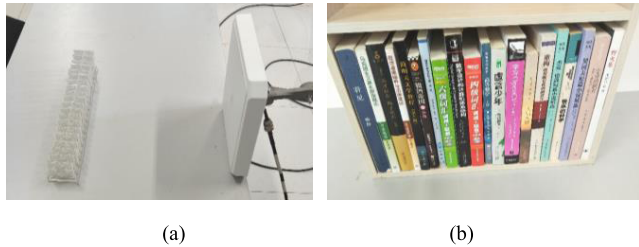


FIGURE 11. Experimental scene.

end of the antenna is flush with the tag sequence, and the moving distance of the antenna is 120 cm. The antenna moves at a speed of 13-15 cm/s, and 2500-3500 ERPT-Files are collected per scan, with an average of 100-200 ERPT-File per tag. On this basis, changing the spacing between tags explores the limits of tag density.

The experimental scene of the book is shown in Figure 10(b). Except that the spacing between the tags is determined by books' thickness, the other parameters are the same as the bare tags. In this actual application scenario, control parameters and variables and explore the influence of the distance between the antenna and the bookshelf and the moving speed of the antenna on the accuracy.

C. EVALUATION CRITERIA

To predict the order of sequence, we first get the left-right relationship of any two tags. On this basis, we can get the order of the sequence through the sorting algorithm. Define the accuracy of determining the left-right relationship of the tags as Relative Accuracy. Besides, define the prediction accuracy of the whole sequence is Absolute Accuracy, which is determined by the longest common subsequence of the predicted and actual sequences, and Relative Accuracy has a significant and direct positive correlation with Absolute Accuracy. If the actual sequence is [1]-[5], and the left-right relationship of 3 and 4 are judged incorrectly, resulting in a prediction sequence of [1]-[5], 1 out of 10 pairs of data is judged incorrectly, then the Relative Accuracy is 9/10 = 0.9. The length of the longest common subsequence of the two is 4, so the Absolute Accuracy is 4/5 = 0.8. The absolute accuracy here is equivalent to the X-axis accuracy defined in STPP and the Z-axis accuracy in HMRL. As an auxiliary evaluation criterion, the Error value is defined as the number of errors in one scan that is the most misjudged in all scanned sequences.

$$Relative\ Accuracy = \frac{\#\ of\ tag\ pairs\ judged\ correctly}{\#\ of\ tag\ pairs\ in\ total}$$

$$Absolute\ Accuracy = \frac{\#\ of\ tags\ ordered\ correctly}{\#\ of\ tags\ in\ total}$$

D. EVALUATION OF BARE TAGS

According to the deployment described in part A, 50 sets of data were scanned, and the training set and test set were divided according to the ratio of 8:2. In the test result, Relative

Accuracy is 0.986, the Absolute Accuracy is 0.991, and the Error value is 1, which means that the PRDL can achieve good results on bare tags.

| ID | 2    | 1    | 3    | 4    | 5    | 6    | 7    | 8    | 9    | 10   | 11   | 12   | 13   | 14   | 15   | 16   | 17   | 18   | 19   | 20   |
|----|------|------|------|------|------|------|------|------|------|------|------|------|------|------|------|------|------|------|------|------|
| 2  | 0.00 | 0.20 | 0.93 | 0.96 | 0.97 | 0.99 | 1.00 | 1.00 | 1.00 | 1.00 | 1.00 | 1.00 | 1.00 | 1.00 | 1.00 | 1.00 | 1.00 | 1.00 | 1.00 | 1.00 |
| 1  | 0.15 | 0.00 | 0.84 | 0.93 | 0.96 | 0.99 | 1.00 | 1.00 | 1.00 | 1.00 | 1.00 | 1.00 | 1.00 | 1.00 | 1.00 | 1.00 | 1.00 | 1.00 | 1.00 | 1.00 |
| 3  | 0.09 | 0.11 | 0.00 | 0.22 | 0.92 | 0.99 | 1.00 | 1.00 | 1.00 | 1.00 | 1.00 | 1.00 | 1.00 | 1.00 | 1.00 | 1.00 | 1.00 | 1.00 | 1.00 | 1.00 |
| 4  | 0.06 | 0.05 | 0.05 | 0.00 | 0.66 | 1.00 | 1.00 | 1.00 | 1.00 | 1.00 | 1.00 | 1.00 | 1.00 | 1.00 | 1.00 | 1.00 | 1.00 | 1.00 | 1.00 | 1.00 |
| 5  | 0.04 | 0.04 | 0.03 | 0.03 | 0.00 | 1.00 | 1.00 | 1.00 | 1.00 | 1.00 | 1.00 | 1.00 | 1.00 | 1.00 | 1.00 | 1.00 | 1.00 | 1.00 | 1.00 | 1.00 |
| 6  | 0.00 | 0.00 | 0.00 | 0.00 | 0.01 | 0.00 | 0.64 | 1.00 | 1.00 | 1.00 | 1.00 | 1.00 | 1.00 | 1.00 | 1.00 | 1.00 | 1.00 | 1.00 | 1.00 | 1.00 |
| 7  | 0.00 | 0.00 | 0.00 | 0.00 | 0.00 | 0.10 | 0.00 | 0.68 | 0.97 | 0.99 | 0.99 | 1.00 | 1.00 | 1.00 | 1.00 | 1.00 | 1.00 | 1.00 | 1.00 | 1.00 |
| 8  | 0.00 | 0.00 | 0.00 | 0.00 | 0.00 | 0.03 | 0.13 | 0.00 | 0.73 | 0.92 | 0.97 | 0.99 | 1.00 | 1.00 | 1.00 | 1.00 | 1.00 | 1.00 | 1.00 | 1.00 |
| 9  | 0.00 | 0.00 | 0.00 | 0.00 | 0.00 | 0.00 | 0.03 | 0.12 | 0.00 | 0.44 | 0.96 | 0.98 | 1.00 | 1.00 | 1.00 | 1.00 | 1.00 | 1.00 | 1.00 | 1.00 |
| 10 | 0.00 | 0.00 | 0.00 | 0.00 | 0.00 | 0.00 | 0.01 | 0.03 | 0.06 | 0.00 | 0.92 | 0.97 | 0.99 | 1.00 | 1.00 | 1.00 | 1.00 | 1.00 | 1.00 | 1.00 |
| 11 | 0.00 | 0.00 | 0.00 | 0.00 | 0.00 | 0.00 | 0.01 | 0.01 | 0.01 | 0.03 | 0.93 | 0.92 | 1.00 | 1.00 | 1.00 | 1.00 | 1.00 | 1.00 | 1.00 | 1.00 |
| 12 | 0.00 | 0.00 | 0.00 | 0.00 | 0.00 | 0.00 | 0.00 | 0.00 | 0.00 | 0.01 | 0.00 | 0.98 | 1.00 | 1.00 | 1.00 | 1.00 | 1.00 | 1.00 | 1.00 | 1.00 |
| 13 | 0.00 | 0.00 | 0.00 | 0.00 | 0.00 | 0.00 | 0.00 | 0.00 | 0.00 | 0.00 | 0.00 | 0.91 | 1.00 | 1.00 | 1.00 | 1.00 | 1.00 | 1.00 | 1.00 | 1.00 |
| 14 | 0.00 | 0.00 | 0.00 | 0.00 | 0.00 | 0.00 | 0.00 | 0.00 | 0.00 | 0.00 | 0.00 | 0.00 | 0.00 | 0.00 | 0.00 | 1.00 | 1.00 | 1.00 | 1.00 | 1.00 |
| 15 | 0.00 | 0.00 | 0.00 | 0.00 | 0.00 | 0.00 | 0.00 | 0.00 | 0.00 | 0.00 | 0.00 | 0.00 | 0.00 | 0.00 | 0.00 | 0.00 | 0.00 | 0.00 | 0.00 | 0.00 |
| 16 | 0.00 | 0.00 | 0.00 | 0.00 | 0.00 | 0.00 | 0.00 | 0.00 | 0.00 | 0.00 | 0.00 | 0.00 | 0.00 | 0.00 | 0.00 | 0.00 | 0.00 | 0.00 | 0.00 | 0.00 |
| 17 | 0.00 | 0.00 | 0.00 | 0.00 | 0.00 | 0.00 | 0.00 | 0.00 | 0.00 | 0.00 | 0.00 | 0.00 | 0.00 | 0.00 | 0.00 | 0.00 | 0.00 | 0.00 | 0.00 | 0.00 |
| 18 | 0.00 | 0.00 | 0.00 | 0.00 | 0.00 | 0.00 | 0.00 | 0.00 | 0.00 | 0.00 | 0.00 | 0.00 | 0.00 | 0.00 | 0.00 | 0.00 | 0.00 | 0.00 | 0.00 | 0.00 |
| 19 | 0.00 | 0.00 | 0.00 | 0.00 | 0.00 | 0.00 | 0.00 | 0.00 | 0.00 | 0.00 | 0.00 | 0.00 | 0.00 | 0.00 | 0.00 | 0.00 | 0.00 | 0.00 | 0.00 | 0.00 |
| 20 | 0.00 | 0.00 | 0.00 | 0.00 | 0.00 | 0.00 | 0.00 | 0.00 | 0.00 | 0.00 | 0.00 | 0.00 | 0.00 | 0.00 | 0.00 | 0.00 | 0.00 | 0.00 | 0.00 | 0.00 |

FIGURE 12. Judgment matrix.

To study the effectiveness of the sorting algorithm, Figure 12 shows the matrix of data processed by the sorting algorithm. The sorting result misjudges the order 1-2 as 2-1, and the red squares represent the wrong judge result of left-right relationship. After employing the sort algorithm, the effects of misjudgment of 0.32 and 0.44 have been eliminated.

After that, the sequence can be visually displayed and corrected. For example, when testing 20 tags, if the correct sequence is set to: [1, 2, 3, 4, 5, 6, 7, 8, 9, 10, 11, 12, 13, 14, 15, 16, 17, 18, 19, 20].. Supposing that the sequence order is adjust to:[1, 5, 3, 2, 4, 6, 8, 9, 10, 7, 11, 12, 13, 14, 16, 15, 17, 18, 19, 20], after the system predicts the current sequence, the longest common subsequence algorithm is used to compare the correct sequence with the current sequence, and then the tags that need to be replaced are found: 5, 3, 7, 16. Correct positions of these tags are marked by Original, as the Figure 13 shows.

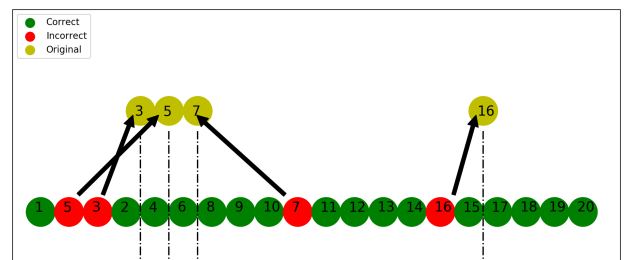


FIGURE 13. Correct sequence visualization.

We further tested the effect of the tag spacing s on the accuracy. STPP has been tested in the range of [2 cm, 10 cm], and the accuracy is more than 90% when the spacing is 8 cm or more, while the effect is very poor at 2cm, with an accuracy of 0.42 for X-axis ordering and 0.23 for Y-axis ordering [10]. HMRL was tested in the range of [5 cm, 40 cm], the effect is poor at 5 cm, and the comprehensive accuracy is above 88.10% when spacing is above 10 cm [12]. Part of the test scenarios of PRDL are shown in Figure 14. The accuracy of PRDL compared with the prior art is shown



FIGURE 14. Partial test scenario.

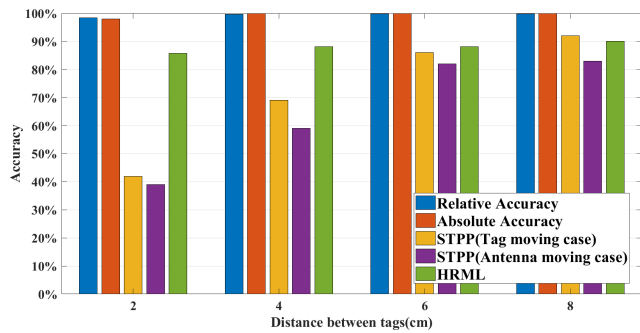


FIGURE 15. Accuracy comparison between PRDL and prior art at different tag densities.

in Figure 15. STPP first proposed the concept of relative localization, which has groundbreaking significance, but there are many shortcomings. The ordering accuracy of STPP decreases dramatically as we slightly narrow the distance between tags, which means that the stability is insufficient. And its accuracy has not made a breakthrough. It can be seen that HMRL has improved on the basis of STPP, and its stability has also made great progress, but the accuracy still has a relatively large room for improvement. It is clear that PRDL performs better in accuracy and stability. We focus on the relative localization of the tags at high density, in our research results, as the distance between tags decreases, the accuracy decreases slowly and remains at a high level. Table 2 gives the test results of PRDL in the range [1cm, 5cm]. PRDL can still achieve accuracy of 0.973 and 0.98 in the case of a high density of 1cm. The experiment of bare tag proves that PRDL has a great breakthrough in the relative localization of high-density tags, and its localization accuracy is remarkable.

TABLE 2. Tag separation distance vs. accuracy.

| Distance between tags | 1 cm  | 2 cm  | 3 cm  | 4 cm  | 5 cm  |
|-----------------------|-------|-------|-------|-------|-------|
| Relative Accuracy     | 0.973 | 0.984 | 0.992 | 0.997 | 0.998 |
| Absolute Accuracy     | 0.98  | 0.98  | 0.99  | 1     | 1     |
| Error value           | 1     | 1     | 1     | 0     | 0     |

E. EVALUATION OF BOOKS

The experimental results of bare tag indicate that PRDL is sufficient for the library’s book arrangement. In the library, the distance between tags is not uniform, but is determined by the thickness of different books, mostly distributed in 1-3 cm, which means that the model trained with the data collected from the isometric bare tags may not do well. So we randomly selected 20 books, and the first page of each book was labeled with an RFID tag. Except for the random parameter s, the experimental parameters were the same with that in the experiment on bare tags. 50 sets of data were collected to perform above-mentioned relative localization of sequences. The training data and test data are for books of the same fixed position order, and the test results are not much different from the bare tags. Minor changes in the distance between the tags do not affect the accuracy of the PRDL too much.

The distribution of books in the library is complex. One of the tasks of the librarian is to arrange books, and situations that need to be handled are various. We did different tests for the different situations, including changing the position of specific books, adding a book, and taking a book. The increase and decrease of books can be easily detected by comparing the EPC code and database data, but the exchange of book positions is not directly detectable. We randomly took a few books to misplace their positions and collected test data separately, and the accuracy does not attain the expected results. We suspect that the training data is too singular, the model is sensitive to the fixed spacing of the books in the training data, so that the detection ability for adjusted book sequence is poor. To solve this problem, we used a large number of books of different thicknesses, and repeatedly randomly disordered the book order, collected 50 sets of data, and added the data to the previous training data to train the final model. We randomly arranged all the books and collected 60 sets of test data that were completely independent of the training data. The final model’s test results are 0.991 for Relative Accuracy, 0.999 for Absolute Accuracy, and 1 for Error value. The final model can be well detected. Books out of order, which is able to detect the order of disorder books well.

We categorized all the test data. Obviously, the larger the interval between the tags, the more obvious the data characteristics. Adjacent tags are necessarily the most difficult to judge, and Figure 16 shows the error rate of tag pairs at different intervals. When the tags are separated by more than 6 tags, the model judgment error rate of the PRDL is 0, except that the error rate of the adjacent tags is 0.16, and the others are all less than 0.06. Even so, Absolute accuracy of the test is very good, mainly because the sorting algorithm has a good correction effect on output data of the model. Therefore, Relative accuracy is the basis of Absolute accuracy, but the Absolute accuracy cannot be completely determined by it.

F. ROBUSTNESS ANALYSIS

In the experiment, the distance between the antenna and the tag sequence and the speed of the antenna movement

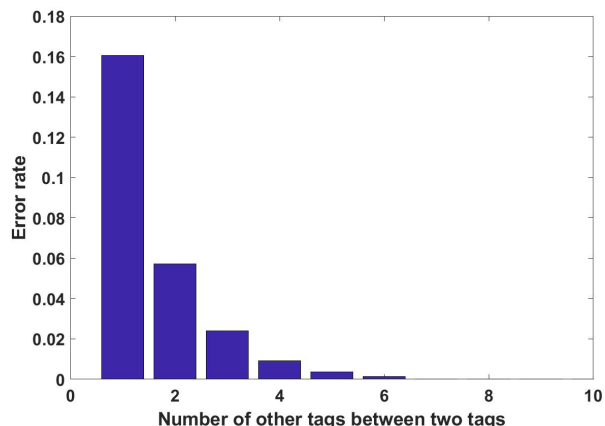


FIGURE 16. Relative accuracy statistics in test data.

TABLE 3. Distance to antenna vs. accuracy.

| Distance to antenna | Relative Accuracy | Absolute Accuracy | Error value |
|---------------------|-------------------|-------------------|-------------|
| -25 cm              | 0.906             | 0.91              | 3           |
| -20 cm              | 0.981             | 1                 | 0           |
| -15 cm              | 0.981             | 1                 | 0           |
| -10 cm              | 0.963             | 0.946             | 2           |
| -5 cm               | 0.957             | 0.99              | 1           |
| -4 cm               | 0.960             | 0.975             | 2           |
| -3 cm               | 0.976             | 0.98              | 1           |
| -2 cm               | 0.986             | 1                 | 0           |
| -1 cm               | 0.988             | 1                 | 0           |
| +1 cm               | 0.991             | 1                 | 0           |
| +2 cm               | 0.989             | 1                 | 0           |
| +3 cm               | 0.981             | 1                 | 0           |
| +4 cm               | 0.967             | 1                 | 0           |
| +5 cm               | 0.955             | 1                 | 0           |
| +10 cm              | 0.956             | 0.975             | 1           |
| +20 cm              | 0.952             | 0.99              | 1           |
| +30cm               | 0.948             | 0.945             | 2           |

are fixed. However, in real applications, these parameters are not completely consistent with the experimental parameters, so we further explored the robustness of the final model, determined acceptable range of parameter deviations and improve the robustness of the model. We changed the distance between the antenna and the tag sequence, the speed of the antenna and the height of the antenna relative to the tag, and then collected the test data. And we just want to explore the robustness of the method, so we sweep these books only about 15 times in each case. Considering the actual situation, we study the parameters within the possible offset range based on the original parameter values, and the results are shown in Table 2, Table 3 and Table 4, where ‘-’ represents the reduction of the original parameter and ‘+’ represents the increase of original parameter.

TABLE 4. Antenna moving speed vs. Accuracy.

| Time(s) | Speed(cm/s) | Relative Accuracy | Absolute Accuracy | Error value |
|---------|-------------|-------------------|-------------------|-------------|
| 6-7 s   | 17-20       | 0.966             | 1                 | 0           |
| 7-8 s   | 15-17       | 0.989             | 1                 | 0           |
| 9-10 s  | 12-13       | 0.987             | 1                 | 0           |

1) ANTENNA DISTANCE TO TAGS VS. ACCURACY

Reader distance to tags was adjusted up and down based on original value of 35 cm, so that its impact on accuracy rate can be found, and the experiment results are shown in Table 5. We first explored within 1-5 cm, and the accuracy rate maintains at a very high level. Next, we further expanded the scope of inquiry. Since the adjustment is based on the original value, the distance reduction value does not exceed 35 cm at most, but because of the thickness of the antenna, in order to move the antenna easily, we take the maximum reduction of the distance of 25 cm; the low-power antenna we used has a limited reading distance, and the maximum distance at which antenna can smoothly read tags is about 75 cm, so the maximum increase of the distance is 30 cm.

TABLE 5. Antenna height vs. accuracy.

| Height | Relative Accuracy | Absolute Accuracy | Error value |
|--------|-------------------|-------------------|-------------|
| 2 cm   | 0.991             | 1                 | 0           |
| 1 cm   | 0.988             | 1                 | 0           |
| -1 cm  | 0.989             | 1                 | 0           |
| -2 cm  | 0.99              | 1                 | 0           |

The experimental results show that, on the one hand, the larger the adjustment of distance is, the lower the accuracy is. Moreover, reducing the Reader distance to tags have a greater impact on the accuracy than increasing it. On the other hand, in the test range, no matter how the distance is adjusted, the accuracy rate can reach above 0.9, even when the distance is extremely large or extremely small, indicating the robustness of the system.

2) ANTENNA MOVING SPEED VS. ACCURACY

During the acquisition of training data, the moving distance of the antenna was set to 120 cm and the moving time was set to 8 s. Due to the error, the actual moving time was 8-9 s and the speed was 13-15 cm/s. On this basis, the movement speed of the antenna was adjusted up and down, and its influence on the accuracy is shown in Table 4. Generally speaking, the larger the adjustment of speed is, the lower the accuracy is. However, the accuracy rate has been maintained at a very high level in the test and its change is not obvious, so the model has generalization ability for speed and has good robustness.

### 3) ANTENNA HEIGHT VS. ACCURACY

Keeping the antenna surface perpendicular to the side of the tag sequence, we adjusted the height of the antenna and collected the test data. The test results are shown in Table 5, which shows that the deviation of height within 2 cm has little effect on the relative localization results. Because PRDL collects data at a specific height, such as moving the antenna on a platform and loading the antenna in a fixed position on the handcart, the height parameters are usually constant and there is no deviation whenever data acquisition is performed. Therefore, it is not necessary to explore the influence of the large deviation on the relative localization results. The experimental results show that the robustness is good in a small deviation range.

## G. SOME DISCUSSIONS ABOUT PRDL

### 1) ADVANTAGES AND DISADVANTAGES

The experimental results show that PRDL is remarkably accurate, and has a huge advantage compared with the existing relative localization technology in terms of accuracy. Moreover, PRDL is a breakthrough in the relative localization of dense tags, although the tag spacing is only 1cm, but still maintain high accuracy. relative localization. PRDL also has certain disadvantages. The main disadvantage is that the work of collecting training data is cumbersome, and the workload of the actual scene deployment is increased. This is a common problem caused by deep learning technology, because most existing deep learning based systems have to deployed according to actual scenarios [24], [25].

### 2) GENERALIZATION

If PRDL collects training data from the actual scene, outputs the model, and is deployed in the corresponding scene, the high detection accuracy of the scene can be guaranteed. For example, in a library scene, an RFID reader and an antenna are loaded in a trolley to make a linear movement between the bookshelves, and the training data is collected when antenna is scanning the tags in the books. In practical applications, data collected in the same way can be used for book sequence detection. Such a model is targeted, but if data of various special situations is added into the training data, the generalization ability of the model can be improved to obtain a better practical application effect.

### 3) OPERATION TIME

When using deep learning to solve practical problems, program run time is an important indicator for evaluating program quality. After all, even if the accuracy of the system is very high, if the running time is too long to achieve real-time, then the system is not very practical. Using the final model for 10,000 times sequence arrangement detection takes only 976 ms, indicating that the system can provide powerful real-time services.

### 4) DEEP NEURAL NETWORK SELECTION

In the selection of deep neural networks, we have tried various networks such as CNN, LSTM [26], and the actual test results have finally selected CNN. This is only the conclusion of our experiment, there must be better solution for optimizing the neural network which requires further research and exploration.

## VI. CONCLUSION

Relative Localization Method of RFID Tags via Phase and RSSI based on Deep Learning (PRDL) proposed in this paper bypasses the inherent problems in absolute localization such as limited accuracy, and creatively applies deep learning to relative localization. Extracting the characteristics of RSSI and Phase as the training data to train model, PRDL achieve precise relative localization of objects. The experimental results show that PRDL has a good effect and has higher accuracy than the existing relative localization methods. This technology can be applied not only to library management, but also to any field where RFID is currently being used for relative localization, such as warehouse cargo localization and supermarket logistics management, which require indoor real-time relative localization. Additionally, when PRDL is using for relative localization of objects, the inventory of object can be carried out at the same time, which means the inventory system can be naturally embedded in the localization system. Meanwhile, if absolute localization is required, the fusion of relative and absolute localization system can also be performed. Currently, the deployment of the RFID system is relatively expensive, so the integration of different systems can reduce deployment costs.

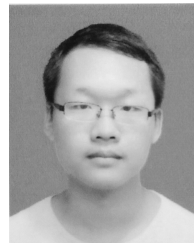
## REFERENCES

- [1] L. Yang, Y. Chen, X.-Y. Li, C. Xiao, M. Lim, and Y. Liu, "Tagoram: Real-time tracking of mobile RFID tags to high precision using COTS devices," in *Proc. 20th Annu. Int. Conf. Mobile Comput. Netw.*, 2014, pp. 237–248.
- [2] L. M. Ni, Y. Liu, Y. C. Lau, and A. P. Patil, "LANDMARC: Indoor location sensing using active RFID," in *Proc. IEEE Int. Conf. Pervasive Comput. Commun.*, Mar. 2003, pp. 407–415.
- [3] Y. Zhang et al., "LANDMARC indoor location algorithm based on quantum particle swarm optimized cubature Kalman filtering," *J. Electron. Meas. Instrum.*, vol. 32, no. 2, pp. 72–79, 2018.
- [4] H. Xu, M. Wu, P. Li, F. Zhu, and R. Wang, "An RFID indoor positioning algorithm based on support vector regression," *Sensors*, vol. 18, no. 5, p. 1504, 2018.
- [5] Y. Fu, C. Wang, R. Liu, G. Liang, H. Zhang, and S. U. Rehman, "Moving object localization based on UHF RFID phase and laser clustering," *Sensors*, vol. 18, no. 3, p. 825, 2018.
- [6] Y. Ma, B. Wang, S. Pei, Y. Zhang, S. Zhang, and J. Yu, "An indoor localization method based on AOA and PDOA using virtual stations in multipath and NLOS environments for passive UHF RFID," *IEEE Access*, vol. 6, no. 6, pp. 31772–31782, 2018.
- [7] J. Zhang, Y. Lyu, J. Patton, S. C. G. Periaswamy, and T. Roppel, "BFVP: A probabilistic UHF RFID tag localization algorithm using Bayesian filter and a variable power RFID model," *IEEE Trans. Ind. Electron.*, vol. 65, no. 10, pp. 8250–8259, Oct. 2018.
- [8] C. Duan, L. Yang, Q. Lin, and Y. Liu, "Tagspin: High accuracy spatial calibration of RFID antennas via spinning tags," *IEEE Trans. Mobile Comput.*, vol. 17, no. 10, pp. 2438–2451, Oct. 2018.
- [9] L. Shangquan, Z. Li, Z. Yang, M. Li, and Y. Liu, "OTTrack: Order tracking for luggage in mobile RFID systems," in *Proc. IEEE INFOCOM*, Apr. 2013, pp. 3066–3074.

- [10] L. Shanguan, Z. Yang, A. X. Liu, Z. Zhou, Y. Liu, "STPP: Spatial-temporal phase profiling-based method for relative RFID tag localization," *IEEE/ACM Trans. Netw.*, vol. 25, no. 1, pp. 596–609, Feb. 2017.
- [11] J. Wang and D. Katabi "Dude, where's my card?: RFID positioning that works with multipath and non-line of sight," *ACM SIGCOMM Comput. Commun. Rev.*, vol. 43, no. 4, pp. 51–62, 2013,
- [12] G. Wang et al., "HMRL: Relative localization of RFID tags with static devices," in *Proc. IEEE Int. Conf. Sens., Commun., Netw.*, Jun. 2017, pp. 1–9.
- [13] T. Nick, J. Goetze, W. John, and G. Stoenner, "Localization of passive UHF RFID labels using an unscented Kalman filter with relative position information," in *Proc. 7th Eur. Workshop Smart Objects, Syst., Technol. Appl.*, 2011, pp. 1–7.
- [14] L. Deng and D. Yu, "Deep learning: Methods and applications," *Found. Trends Signal Process.*, vol. 7, nos. 3–4, pp. 197–387, Jun. 2014.
- [15] L. Shen, Q. Zhang, G. Cao, and He Xu, "Fall detection system based on deep learning and image processing in cloud environment," in *Proc. Conf. Complex, Intell., Softw. Intensive Syst.*, Cham, Switzerland: Springer, 2018, pp. 590–598.
- [16] X. Glorot, A. Bordes, and Y. Bengio, "Domain adaptation for large-scale sentiment classification: A deep learning approach," in *Proc. 28th Int. Conf. Mach. Learn.*, 2011, pp. 513–520.
- [17] D. E. Grzechca, P. Pelczar, and L. Chruszczyk, "Analysis of object location accuracy for iBeacon technology based on the RSSI path loss model and fingerprint map," *Int. J. Electron. Telecommun.*, vol. 62, no. 4, pp. 371–378, 2016.
- [18] J. T. Shen, "Research of logarithmic distance path loss model based on RSSI," *Electron. Quality*, vol. 12, no. 1, pp. 15–17, 2013.
- [19] C. C. Zou, G. J. Hong, and H. Y. Yan, "Effect of different data standardization methods on spectrum-effect relationship for anticoagulation of *Trichosanthis Fructus* dropping pills," *Zhongguo Zhong Yao Za Zhi*, vol. 43, no. 9, pp. 1864–1870, 2018.
- [20] Z. Liu, J. Hu, L. Weng, and Y. Yang, "Rotated region based CNN for ship detection," in *Proc. IEEE Int. Conf. Image Process.*, Sep. 2017, pp. 900–904.
- [21] Y. Guo, J. Zhang, J. Cai, B. Jiang, and J. Zheng, "CNN-based real-time dense face reconstruction with inverse-rendered photo-realistic face images," *IEEE Trans. Pattern Anal. Mach. Intell.*, to be published. doi: 10.1109/TPAMI.2018.2837742.
- [22] F.-C. Chen and M. R. Jahanshahi, "NB-CNN: Deep learning-based crack detection using convolutional neural network and Naïve Bayes data fusion," *IEEE Trans. Ind. Electron.*, vol. 65, no. 5, pp. 4392–4400, May 2018.
- [23] *Impinj*. Accessed: Aug. 2018. [Online]. Available: <http://www.impinj.com>
- [24] E. Gibson et al., "NiftyNet: A deep-learning platform for medical imaging," *Comput. Methods Programs Biomed.*, vol. 158, pp. 113–122, May 2018.
- [25] L.-S. Chen et al., "A Web-based dynamic user customized entry system for public health surveillance," *J. Exp. Clin. Med.*, vol. 5, no. 1, pp. 37–41, 2013.
- [26] K. Greff, R. K. Srivastava, J. Koutník, B. R. Steunebrink, and J. Schmidhuber, "LSTM: A search space odyssey," *IEEE Trans. Neural Netw. Learn. Syst.*, vol. 28, no. 10, pp. 2222–2232, Oct. 2017.
- [27] B. Shi, X. Bai, and C. Yao, "An end-to-end trainable neural network for image-based sequence recognition and its application to scene text recognition," *IEEE Trans. Pattern Anal. Mach. Intell.*, vol. 39, no. 11, pp. 2298–2304, Nov. 2017.
- [28] X. Fu, E. Ch'ng, U. Aickelin, and S. See, "CRNN: A joint neural network for redundancy detection," in *Proc. IEEE Int. Conf. Smart Comput.*, May 2017, pp. 1–8.
- [29] X. Shi, Z. Chen, H. Wang, D.-Y. Yeung, W.-k. Wong, and W.-C. Woo, "Convolutional LSTM Network: A machine learning approach for precipitation nowcasting," in *Proc. Int. Conf. Neural Inf. Process. Syst.*, Cambridge, MA, USA: MIT Press, 2015, pp. 802–810.
- [30] D. M. Dobkin, *The RF in RFID: Passive UHF RFID in Practice*. Burlington, MA, USA: Newton, 2007.
- [31] H. Lehpamer, *RFID Design Principles*. Norwood, MA, USA: Artech House, 2008.
- [32] W. A. Davis and W. L. Stutzman, *Antenna Theory*. Hoboken, NJ, USA: Wiley, 1999.
- [33] C. A. Balanis, "Antenna theory: Analysis and design," *IEEE Antennas Propag. Soc. Newslett.*, vol. 24, no. 6, pp. 28–29, 2003.



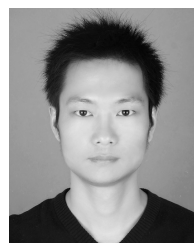
**LEIXIAN SHEN** is currently pursuing the bachelor's degree in software engineering with the School of Computer Science, Nanjing University of Posts and Telecommunications, Nanjing, Jiangsu, China. His research interests include the Internet of Things and artificial intelligence technology.



**QINGYUN ZHANG** is currently pursuing the bachelor's degree in software engineering with the School of Computer Science, Nanjing University of Posts and Telecommunications, Nanjing, Jiangsu, China. His research interests include the Internet of Things and artificial intelligence technology.



**JIAYI PANG** is currently pursuing the bachelor's degree in software engineering with the School of Computer Science, Nanjing University of Posts and Telecommunications, Nanjing, Jiangsu, China. Her research interests include the Internet of Things and artificial intelligence technology.



**HE XU** received the Ph.D. degree in information network from the Nanjing University of Posts and Telecommunications, in 2012, where he is currently an Associate Professor with the School of Computer Science. He is also a Research Staff of Jiangsu High Technology Research Key Laboratory for Wireless Sensor Networks. His research interests include information security and the Internet of Things.



**PENG LI** received the Ph.D. degree from the Nanjing University of Posts and Telecommunications, in 2013, where he is currently an Associate Professor. He is also a Research Staff of Jiangsu High Technology Research Key Laboratory for Wireless Sensor Networks. His main research interests include computer communication networks and information security.